International Journal of Electrical and Computer Engineering (IJECE)
Vol. 12, No. 5, October 2022, pp. 5063~5072
ISSN: 2088-8708, DOI: 10.11591/ijece.v12i5.pp5063-5072

Performance analysis of compressive sensing recovery algorithms for image processing using block processing

Mathiyalakendran Aarthi Elaveini[1], Deepa Thangavel[2]
[1]Department of Electronics and Communication Engineering, SRM Institute of Science and Technology, Ramapuram, India
[2]Department of Electronics and Communication Engineering, SRM Institute of Science and Technology, Kattankulathur, India

Article Info

Article history:

Received Jun 10, 2021
Revised May 23, 2022
Accepted Jun 14, 2022

Keywords:

Basis pursuit
Compressive sampling
matching pursuit
Iterative hard threshold
Iterative reweighed least square
Mean square error
Peak signal to noise ratio
Recovery algorithm

ABSTRACT

The modern digital world comprises of transmitting media files like image, audio, and video which leads to usage of large memory storage, high data transmission rate, and a lot of sensory devices. Compressive sensing (CS) is a sampling theory that compresses the signal at the time of acquiring it. Compressive sensing samples the signal efficiently below the Nyquist rate to minimize storage and recoveries back the signal significantly minimizing the data rate and few sensors. The proposed paper proceeds with three phases. The first phase describes various measurement matrices like Gaussian matrix, circulant matrix, and special random matrices which are the basic foundation of compressive sensing technique that finds its application in various fields like wireless sensors networks (WSN), internet of things (IoT), video processing, biomedical applications, and many. Finally, the paper analyses the performance of the various reconstruction algorithms of compressive sensing like basis pursuit (BP), compressive sampling matching pursuit (CoSaMP), iteratively reweighted least square (IRLS), iterative hard thresholding (IHT), block processing-based basis pursuit (BP-BP) based on mean square error (MSE), and peak signal to noise ratio (PSNR) and then concludes with future works.

Corresponding Author:

Deepa Thangavel
Department of Electronics and Communication Engineering, SRM Institute of Science and Technology
Kattankulathur, Chennai-603203, India
Email: deepat@srmist.edu.in

1. INTRODUCTION

The digital revolution of the internet and social media leads to the transmission of many multimedia signals over the internet. Compression plays a vital role in limiting the bandwidth and storage space of multimedia signals like image audio and video. In 2004, David Donoho and his team proposed compressive sensing a signal sampling theory with captures the signal efficiently and the signal is recovered back with fewer samples thus reducing the dimensionality of signals known as sparse or compressible [1]–[3].

In traditional sampling, the signals are sampled and then compressed whereas in compressive sensing the signals are based on the signal sparsity [4]. Sparsity is a property of an image with most of the elements is zero and the image can be represented by a few non-zero elements image. The sparsity of the matrix is the ratio of zero value elements to the total number of elements. A sparse basis matrix [5] can be obtained from the traditional matrixes like discrete wavelet transform (DWT), discrete cosine transform (DCT), and discrete Fourier transform (DFT). For example, natural images are highly sparse in wavelet while speech signal and medical images have sparsity representation Fourier and random transform [6]. Let X be the original image with NxN matrix elements [7] which is transformed into transform data Y then Y can be expressed as (1).

$$Y = \psi(X) \quad (1)$$

If the entries in matrix Y are close to zero then X is said to be sparse on some basis ψ.

The acquisition model [8] can be mathematically represented as Y= ψ X where X is input signal of size N, ψ is random measurement matrix of size *MxN* and Y is the measurement vector of size M. At the processing end of the reconstruction model [9], the measurement vector Y and reconstruction matrix Θ is space basis X then X is (2).

$$x = \sum_{i=1}^{n} S_i \psi_i \quad (2)$$

Let K be sparsity vector S [10], [11], then the matrix must satisfy restricted isometry property (RIP) and for reconstruction, the measurement matrix ψ and sparse basis should be incoherent [12].

2. RELATED WORKS

The image compression system presented in [13] uses the different techniques for the choice of image compression techniques and for setting up a compression ratio. The image compression was carried out in phases where the first step was to compress the image using DCT, the second to reconstruct, and finally to train a set of images. The paper discusses the design of image compressed sensing (CS) to reduce redundancy based on objective criteria and subjective criteria.

The hardware implementation of CS in [14] was done in field-programmable gate array (FPGA) which is the best platform for reconfigurability. The image was stored in synchronous dynamic random-access memory (SDRAM) and a sparse matrix is generated using the transformation process. The recovery of the image was found to be more complex and time-consuming.

An efficient compression scheme in wireless sensor network (WSN) proposed in [15], [16] presents a new architecture and protocol to achieve energy efficiency and transmit the image over WSN the architecture optimizes high speed in image compression implemented with limited hardware and the power consumption is low. The literature [17], [18] presents the image packet queue to minimize error rate and thus improving the throughput of image transmission. The block compressive sensing proposed in [19] divides the image into blocks thereby maximizing the sparsity and employs an adaptive threshold thereby allocating measurements based on the sparsity of individual blocks with a predetermined measurement ratio.

3. STATE-OF-THE-ART COMPRESSIVE SENSING

Signal and image processing systems rely on the recovery of signals from the information [20]. When the signal acquired is linear, then it can be solved using the linear system equations mathematically as (3):

$$Y = Ax \quad (3)$$

where Y is observed data, which is ϵC^{m} and connected to $X \epsilon C^{\mathrm{N}}$.

The matrix $A \epsilon C^{\mathrm{mxN}}$ is the measurement matrix. Traditionally the number of measurements m should be as large as N. If $m<N$ then the linear system is underdetermined with infinite solution, which makes recovery of X from Y impossible. The above technology is related to the Shannon sampling theorem. Figure 1 shows the block diagram of the compressive sensing and also describes the acquisition model as well as the reconstruction model. The reconstruction algorithms that make this underlying assumption possible is sparsity as shown in Figure 1.

3.1. Acquisition model

The measurement of the signal is made randomly [21] by different techniques like random modulator, modulated wideband converter (MWC), random modulation pre-integrator (RMPI), random filtering, random convolution compressive multiplexer, random equivalent sampling, random triggering based modulated wideband compressive sampling, and quadrature analog to information converter. The proposed a compressive sampler, random [22] which samples the signals below the Nyquist rate. The low pass filter (LPF) results in a unique frequency signature in the low region. The high-frequency signal lies in the low-frequency region. This unique frequency signature gives the original signal in random measurements and finds its application for wideband signal acquisition. MWC uses a parallel architecture. The input signal is multiplexed by different chipping sequences and then passed via LPF thus sampled below the Nyquist rate and can be used for the wideband signal. RMPI is a combination of MWC with a parallel version [23] of random and only the difference is RMPI uses integrator instead of LPF by which the resultant is a different reconstruction method that helps in acquiring the ultrawideband signal. The random filtering method performs convolution with finite impulse response (FIR) and it finds its application in compressing continuous and streaming signals. The random convolution consists of random pulses and then the pulses are obtained by a circular shift of the first row and can be used as a universal acquisition. In compressive multiplexer, the parallel architecture samples multichannel data to obtain a sub-Nyquist rate.

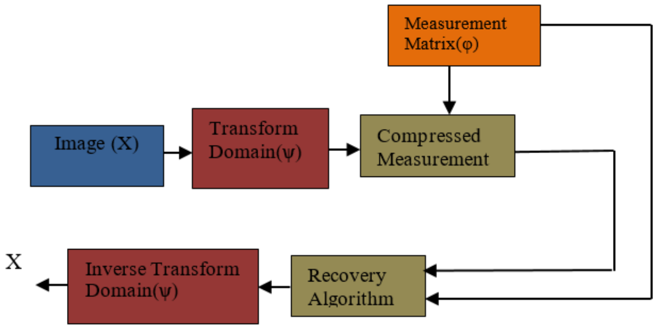

Figure 1. Block diagram for compressive sensing

3.2. Measurement matrix

The measurement matrix plays a vital in compressing the signal, therefore choosing a measurement matrix is important for accuracy and less processing time to recover the signal [24]. Figure 2 gives the different types of measurement matrices deployed for compressive sensing. It is broadly classified into the deterministic and random matrix.

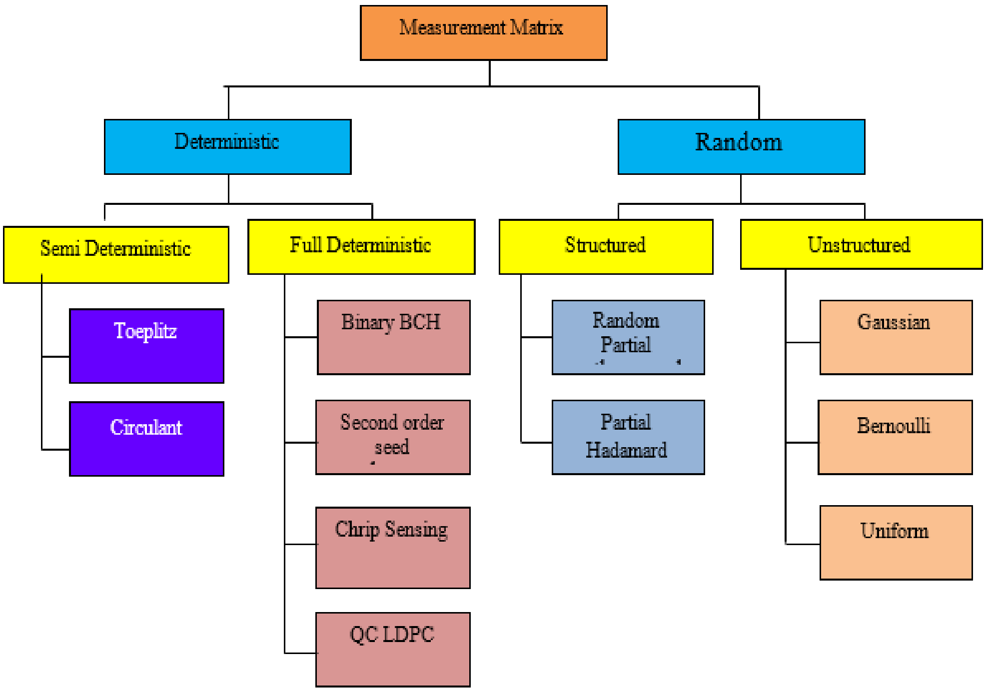

Figure 2. Different types of measurement matrix

a. Random matrix

Random matrices are identical and independent matrices that are generated by the distribution like normal, random, and Bernoulli functions. The random matrix is broadly classified into structured and unstructured matrix unstructured matrices are generated randomly. This matrix includes Gaussian, Bernoulli, and uniform matrix.

b. Gaussian matrix

The elements are distributed normally and the elements are independent except 0 and σ^2 (variance). The probability distribution function is (4).

$$f\left(\frac{1}{\mu},\sigma^2\right)=\frac{1}{\sqrt{2\sigma^2\pi}}\frac{exp(1-\mu^2)}{2\sigma^2} \quad (4)$$

Where μ is mean, σ is standard deviation, and σ^2 is variance.

$$K \le C_1 N\, log\left(\frac{L}{S}\right)+C_2\, log\,\varepsilon-1 \quad (5)$$

Where S is sparsity, N is No. of measurements, L is length of sparse, and C_1, C_2 is circulant matrix.

c. Bernoulli matrix

Bernoulli matrix denoted as $B\epsilon R,\ mxn$ have equal probabilities at $-\frac{1}{\sqrt{m}} or \frac{1}{\sqrt{m}}$, with outcomes n=0 and n=1. The PDF of the Bernoulli matrix is

$$F(n)=\begin{Bmatrix}\frac{1}{2} forn=0\\ \frac{1}{2} forn=1\end{Bmatrix} \text{Which satisfies RIP} \quad (6)$$

d. Structured random matrices

Unstructured matrices are slow and not advisable for large-scale problems since structured matrices follow a structure [25] this reduces storage time and randomness.

e. Random partial Fourier matrix

Consider the matrix F NxN whose entry is

$$(F)_{kj}=exp\frac{2\pi ikj}{N} \quad (7)$$

and k,j takes the value of $\{1,2\ \ldots N\}$. The restricted isometric property (RIP) is also satisfied for the material by randomly choosing M rows $M\ge CK\,log\,N\,/\,\epsilon$. Where M is No. of measurements, K is sparsity, and N is length of sparse signal.

f. Random partial Hadamard matrix

The entries are 1 and -1 for the Hadamard matrix and the column is orthogonal. Consider a matrix H with order *n*, Then $H.\ H^T=NI_N$. Where I_N is Identity matrix and H^T is transpose of H.

g. Deterministic matrices

The matrix follows a deterministic condition for satisfying the RIP. They are divided into semi-deterministic and full-deterministic.

h. Semi-deterministic matrix

Semi-deterministic matrices are generated in two steps. The first column is generated randomly and the full matrix is generated by applying a transformation to the first column thus generating the rows of the matrix.

i. Circulant matrix

The entry for the matrix is $C_j=C_j-I$, where $C=(c_1\ c_2\ \ldots c_n)$ and $i,j=\{1\ \ldots\ N\}$ thus the resultant matrix is circulant.

$$C=\begin{bmatrix} C_n & C_{n-1}\cdots\cdots & C_1\\ C_1 & C_n\cdots\cdots & C_2\\ \vdots & & \\ C_{\ n-1} & C_{n-2} & C_n\end{bmatrix} \quad (8)$$

j. Toeplitz matrix

The resultant Toeplitz matrix T is associated with $t=(t_1,t_2\ldots t_n)$, $T_{ij}=t_{j-i}$ with constant diagonal $T_{ij}=t_{j+1\ j+1}$.

$$T=\begin{bmatrix} t_n\ddots & t_{n-1}\cdots\cdots & t_1\\ t_{n+1} & t_n\cdots\cdots & t_2\\ \vdots & & \\ t_{2n-1} & t_{2n-2}\cdots\cdots & t_n\end{bmatrix} \quad (9)$$

k. Full deterministic matrices

The matrices are purely based on RIP properly.

l. Chirp sensing matrix

The matrix is based on non-cyclic codes where the columns are generated by chirp signal. The matrix of the chirp is given by $A_{chrip} = [u_{r1}\, u_{r2}\, u_{r3} \dots u_{rw}]$ and $U_{rt} = (t = 1 \dots w)$ with MxM matrix.

m. Binary BCH matrices

Binary Bose Chaudhuri Hocquenghem (BCH) matrix is a cyclic matrix and given by (10).

$$H = \begin{bmatrix} 1 & \alpha & \alpha^2 \cdots & \alpha^{(n-1)} \\ 1 & \alpha^3 & \alpha^3 \cdots & \alpha^{3(n-1)} \\ \vdots & \vdots & \vdots\ \vdots & \vdots \end{bmatrix} \quad (10)$$

3.3. Recovery algorithm

The recovery of the original signal after compression is the essential step of compressive sensing. The recovery algorithms are classified into six different categories as shown in Figure 3. Incoherence and RIP are two important factors for the reconstruction of the compressed signal. The maximum correlation between two elements in a pair of matrices is incoherent that involves quantity to measure the suitability of φ [26]. Let the measurement metrics φ and sparse basis Ψ are said to be incoherent to each other. The coherence range is $\psi[\varphi, \psi] \in [1, \sqrt{n}]$. The recovery is better when coherence is small. Let the sparsity of vector S be K, then, to recovery from measurements *Y* [27] the matrix should satisfy RIP with order *K*

$$1 - \delta \le \frac{\|\Theta_U\|_2}{\|U\|_2} \le 1 + \delta \quad (11)$$

$\ell 1$ is minimization or basis pursuit (BP). The convex optimization searches for a minimum $\ell 1$ norm solution. The BP [28] recovers the signal only if its measurement is free from noise.

a. Algorithm for BP

```
Input: A, Y where A-measurement matrix, Y-measurement vector
Instruction: X=argmin‖Z‖, subject to AZ=Y
Output: vector x+
```

b. Greedy pursuit (GP)

Step by step method is implemented in greedy approach [28] and each iteration is selected by updated columns that are similar to measurements.

c. Orthogonal matching pursuit (OMP)

The algorithm is described as

```
Input: A, Y where A-measurement matrix, Y-measurement vector
Initialization: s0=Φ; x0=0
Sn+1=SnU{jn +1} jn+1=argmax {‖A(Y − Ax)‖}
Xn+1=argmin{‖Y − Az‖} supp ZCSn+1
Output:=x+=xn
```

d. Compressive sampling (CoSaMP)

Parallel greedy algorithm not only selects by one atom but operates by selecting *K* or multiplies of *K*. CoSaMP selects *2K* column of measurement matrix which will be added to previous *k* atoms and out of this *3K* atoms the best *K* atoms are taken and updated. Subspace pursuit (SP) [29] selects only *K* atoms for each iteration which reduces the complexity.

e. Threshold approach

The solution set Si is updated using threshold operation. The iterative hard threshold (IHT) [30] uses a non-linear threshold operator ηk keeping the largest *k* entries in *S* all others are set to zero.

$$S = \eta k(s + \lambda \odot T(Y - \odot s) \quad (12)$$

Where λ-denotes step size, if the step size is fixed the algorithm will not recover while step size is adaptive [31] it becomes complicated.

f. Combinal approach

The algorithms make use of two methods count min and count median. In the count min method, it computes the minimum value from a measurement of the previous step. In the count median, the median is calculated instead of the minimum value.

g. Convex approach

The ℓ p norm approach is replaced in the place of ℓ1 norm where 0<p<1 and thus approach recovers the signal from the fewer components. A weaker version of RIP is enough to reconstruct the signal perfectly.

h. Bayesian approach

The Bayesian approach is suitable for signals of a probability distribution. The signals coefficients determining using maximum likelihood estimate or maximum posterior estimate.

i. Block processing-based basis pursuit (BP-BP)

The proposed basis pursuit along with block processing process the image using mean and standard deviation and based on the processed image, the measurement matrix and the DCT transform are performed. The processed image is then recovered using BP and the compression ratio is better when compared to other algorithms.

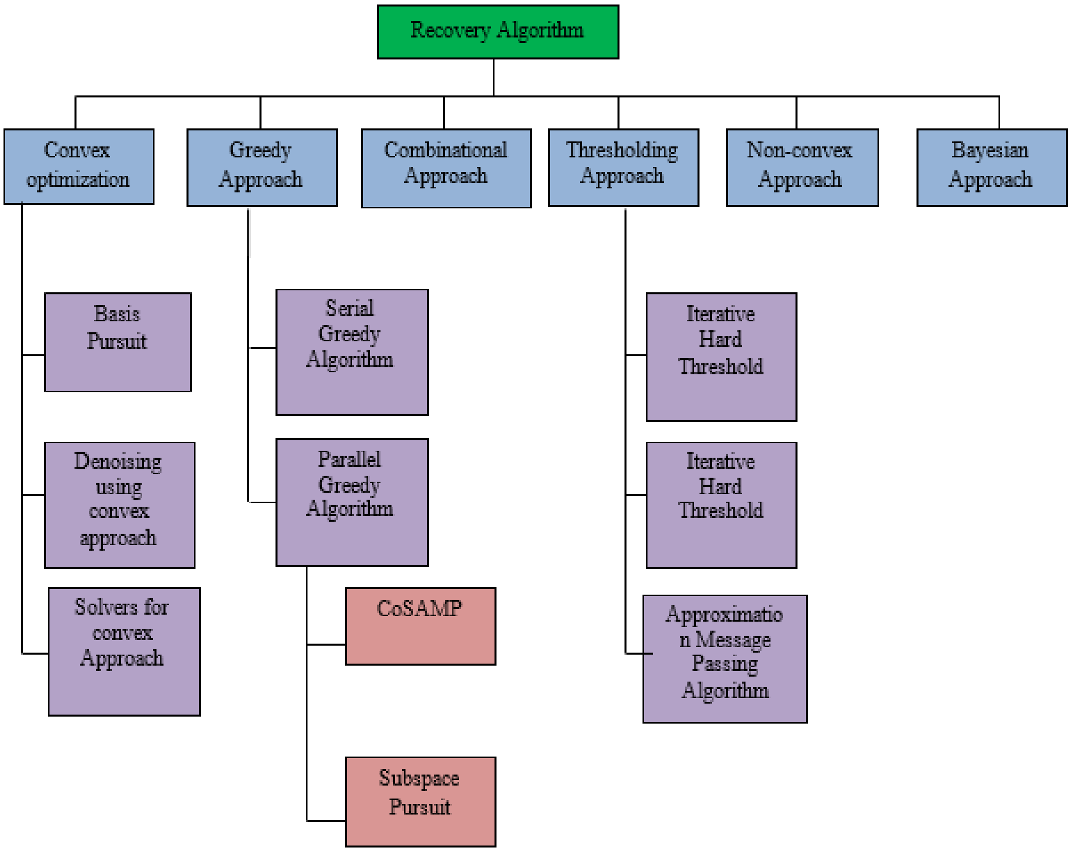

Figure 3. Classification of recovery algorithms

4. RESULT AND DISCUSSION

The various recovery algorithms are analyzed by simulating the output for two different images, cameraman and Lena images. The peak signal to noise ratio (PSNR) and MSE of both the images for various algorithms are tabulated. The peak signal to noise ratio describes the quality metrics of the image. The PSNR is expressed as the ratio of the maximum value of the signal to the noise and it is expressed in the logarithmic decibel scale. PSNR is also defined in terms of MSE. MSE is defined as (13), (14), and (15).

$$MSE = \frac{1}{mn}\sum_{i=0}^{m-1}\sum_{j=0}^{n-1}[I(i,j) - K(i,j)] \quad (13)$$

$$PSNR = 10 \, log \, 10 \left(\frac{Max^2}{MSE}\right) \quad (14)$$

$$PSNR = 20 \, log \, 10 \left(\frac{Max^2}{\sqrt{MSE}}\right) \quad (15)$$

Figure 4 shows the images of the cameraman, which was originally taken for compression, measurement matrix, the compressed image, and the recovered image with the calculated PSNR. Figure 5 gives the comparison of various recovery algorithm for the image's cameraman and Lena at compression ratio 3:1. The PSNR and the MSE for the images are calculated and the tabulation of the images along with their recovery algorithms is tabulated in Table 1.

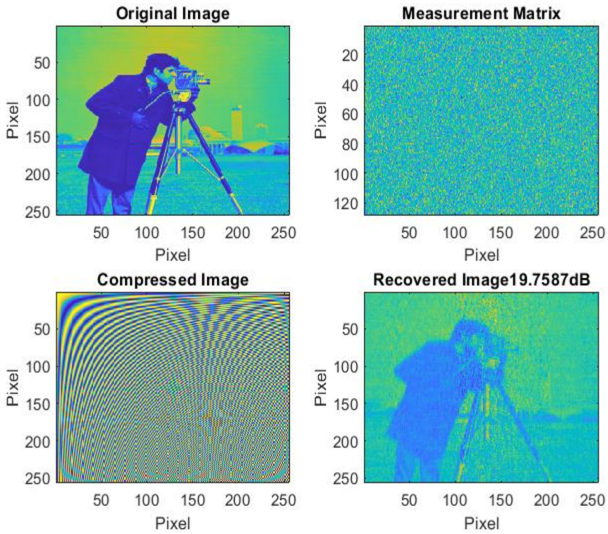

Figure 4. Images of cameraman compressed and recovered

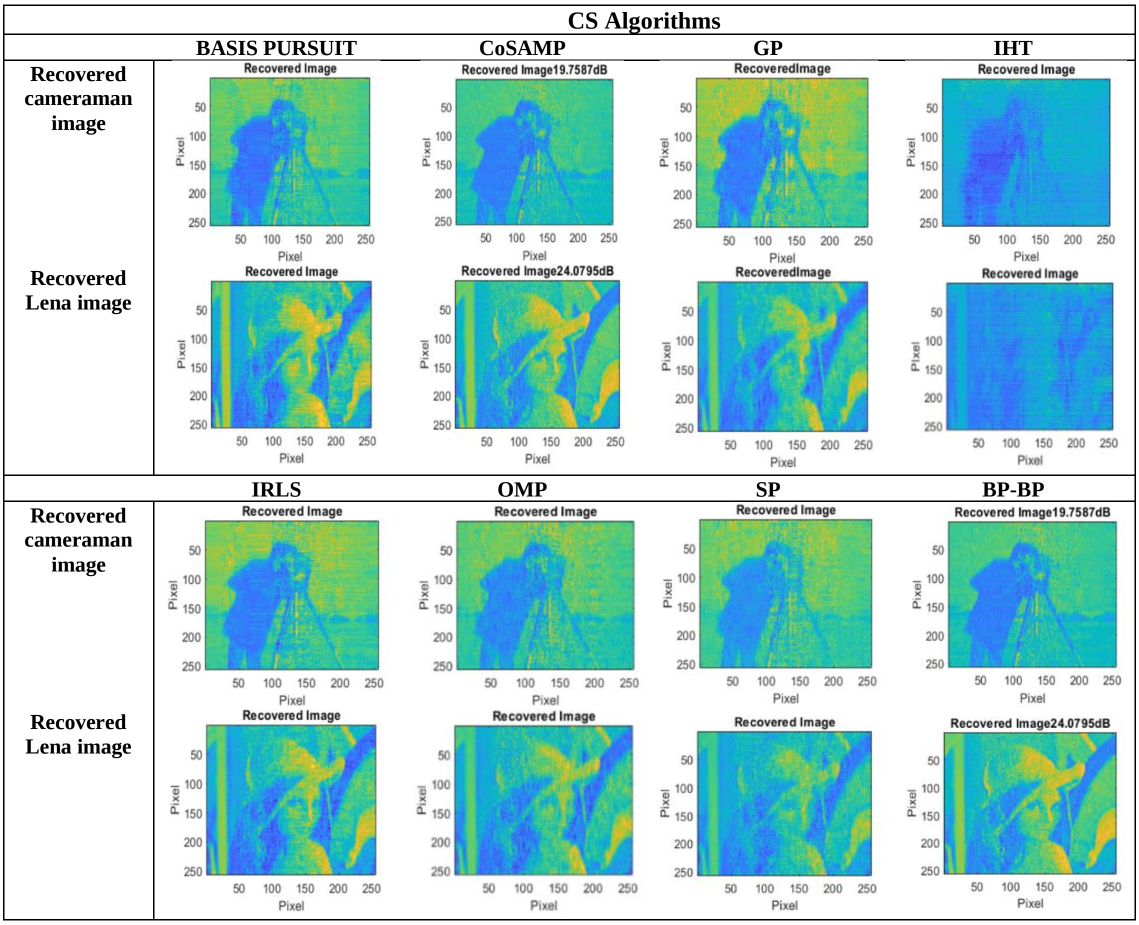

Figure 5. Recovered images of cameraman and Lena with various recovery algorithms

Table 1. Comparison table of various recovery algorithms, PSNR, and MSE

CS Algorithm	Cameraman		Lena	
	MSE	PSNR in dB	MSE	PSNR in dB
BP	26.14	19.79	18.12	22.97
CoSamp	40.09	16.07	26.50	19.67
GP	29.64	18.69	20.66	21.83
IHT	44.40	15.18	37.86	16.57
IRLS	23.69	16.67	23.69	16.67
OMP	32.08	18.01	20.03	22.10
SP	34.66	17.34	22.30	21.16
BP-BP	26.04	19.80	18.10	23.01

Figures 6 and 7 provide the comparison chart of MSE and PSNR in dB for different images with different recovery algorithm. The results of various algorithms with two different images conclude that based on the sparsity of the images the recovery algorithms reconstruct the image with a compression ratio of 3:1 which means 30% of the data are compressed and thus limits the storage and bandwidth of the system.

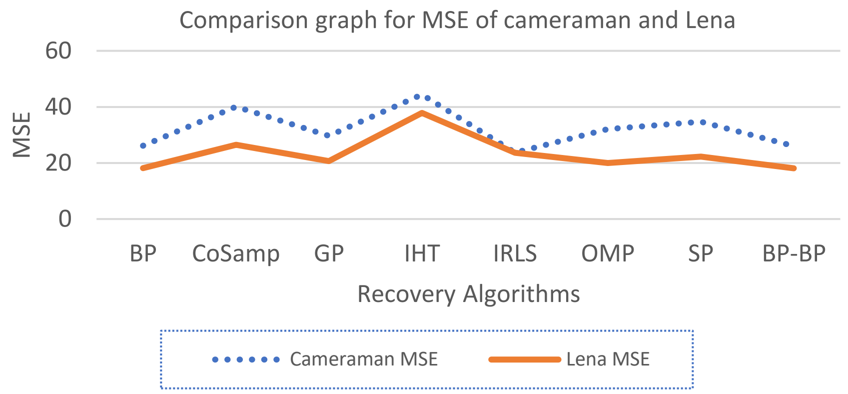

Figure 6. Comparison chart for mean square error

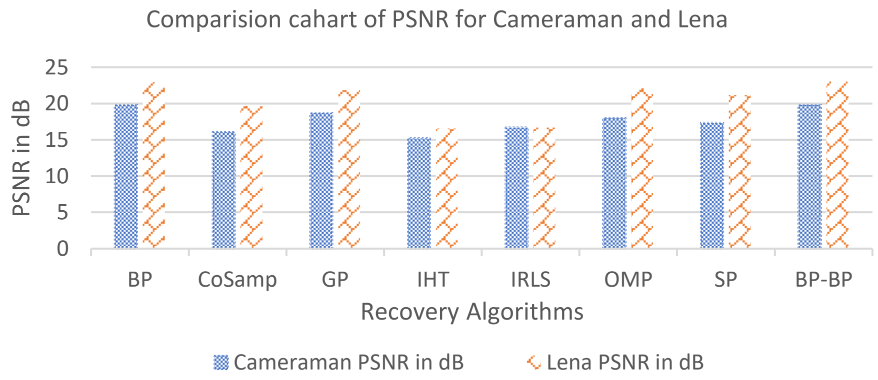

Figure 7. Comparison chart for PSNR

5. CONCLUSION AND FUTURE WORK

The various compressive sensing recovery algorithms are compared and based on their analysis of comparison the recovery of the image depends on the measurement matrix used and the nature of the image. The proposed block processing along with Basis Pursuit is comparatively better in performance than the other algorithms and the compression ratio of the algorithms is found to be 3:1 which is a moderate compression ratio. Based on the present comparison the future work can be enhanced by compressing the image and transmitting the image through a wireless network thereby reducing the storage capacity and transmission rate.

REFERENCES

[1] M. Rani, S. B. Dhok, and R. B. Deshmukh, “A systematic review of compressive sensing: Concepts, implementations and applications,” *IEEE Access*, vol. 6, pp. 4875–4894, 2018, doi: 10.1109/ACCESS.2018.2793851.

[2] D. L. Donoho, “Compressed sensing,” *IEEE Transactions on Information Theory*, vol. 52, no. 4, pp. 1289–1306, Apr. 2006, doi: 10.1109/TIT.2006.871582.

[3] S. Mallat, *A wavelet tour of signal processing: The sparse way*, 3rd ed. Burlington. MA, USA: academic, 2009.

[4] Z. Gao, L. Dai, W. Dai, B. Shim, and Z. Wang, “Structured compressive sensing-based spatio-temporal joint channel estimation for FDD massive MIMO,” *IEEE Transactions on Communications*, vol. 64, no. 2, pp. 601–617, Feb. 2016, doi: 10.1109/TCOMM.2015.2508809.

[5] C. J. Colbourn, D. Horsley, and C. McLean, “Compressive sensing matrices and hash families,” *IEEE Transactions on Communications*, vol. 59, no. 7, pp. 1840–1845, Jul. 2011, doi: 10.1109/TCOMM.2011.051811.100444.

[6] E. J. Candes and M. B. Wakin, “An introduction to compressive sampling,” *IEEE Signal Processing Magazine*, vol. 25, no. 2, pp. 21–30, Mar. 2008, doi: 10.1109/MSP.2007.914731.

[7] Z. Gao, L. Dai, S. Han, C.-L. I, Z. Wang, and L. Hanzo, “Compressive sensing techniques for next-generation wireless communications,” *IEEE Wireless Communications*, vol. 25, no. 3, pp. 144–153, Jun. 2018, doi: 10.1109/MWC.2017.1700147.

[8] M. Lakshminarayana and M. Sarvagya, “MICCS: A novel framework for medical image compression using compressive sensing,” *International Journal of Electrical and Computer Engineering (IJECE)*, vol. 8, no. 5, pp. 2818–2828, Oct. 2018, doi: 10.11591/ijece.v8i5.pp2818-2828.

[9] R. Gribonval and M. Nielsen, “Sparse representations in unions of bases,” *IEEE Transactions on Information Theory*, vol. 49, no. 12, pp. 3320–3325, Dec. 2003, doi: 10.1109/TIT.2003.820031.

[10] R. Chartrand and V. Staneva, “Restricted isometry properties and nonconvex compressive sensing,” *Inverse Problems*, vol. 24, no. 3, 2008.

[11] L. Dai, B. Wang, Y. Yuan, S. Han, I. Chih-lin, and Z. Wang, “Non-orthogonal multiple access for 5G: solutions, challenges, opportunities, and future research trends,” *IEEE Communications Magazine*, vol. 53, no. 9, pp. 74–81, Sep. 2015, doi: 10.1109/MCOM.2015.7263349.

[12] A. Amirjanov and K. Dimililer, “Image compression system with an optimisation of compression ratio,” *IET Image Processing*, vol. 13, no. 11, pp. 1960–1969, Sep. 2019, doi: 10.1049/iet-ipr.2019.0114.

[13] A. M. Joshi, C. Sahu, M. Ravikumar, and S. Ansari, “Hardware implementation of compressive sensing for image compression,” in *TENCON 2017 - 2017 IEEE Region 10 Conference*, Nov. 2017, pp. 1309–1314, doi: 10.1109/TENCON.2017.8228060.

[14] D. M. Pham and S. M. Aziz, “An energy efficient image compression scheme for wireless sensor networks,” in *2013 IEEE Eighth International Conference on Intelligent Sensors, Sensor Networks and Information Processing*, Apr. 2013, pp. 260–264, doi: 10.1109/ISSNIP.2013.6529799.

[15] G. Quer, R. Masiero, G. Pillonetto, M. Rossi, and M. Zorzi, “Sensing, compression, and recovery for WSNs: Sparse signal modeling and monitoring framework,” *IEEE Transactions on Wireless Communications*, vol. 11, no. 10, pp. 3447–3461, Oct. 2012, doi: 10.1109/TWC.2012.081612.110612.

[16] L. Ivan, W. Shaw, and X. Fan, “Wireless multimedia sensor networks,” in *Guide to wireless sensor networks*, Springer, London, 2009, pp. 561–582.

[17] S. Misra, M. Reisslein, and G. Xue, “A survey of multimedia streaming in wireless sensor networks,” *IEEE Communications Surveys & Tutorials*, vol. 10, no. 4, pp. 18–39, 2008, doi: 10.1109/SURV.2008.080404.

[18] Z. Wang and S. Chen, “Performance comparison of image block compressive sensing based on chaotic sensing matrix using different basis matrices,” in *2017 2nd International Conference on Image, Vision and Computing (ICIVC)*, Jun. 2017, pp. 620–623, doi: 10.1109/ICIVC.2017.7984630.

[19] C. Luo, J. Sun, and F. Wu, “Compressive network coding for approximate sensor data gathering,” in *2011 IEEE Global Telecommunications Conference - GLOBECOM 2011*, Dec. 2011, pp. 1–6, doi: 10.1109/GLOCOM.2011.6134085.

[20] C. Luo, F. Wu, J. Sun, and C. W. Chen, “Efficient measurement generation and pervasive Sparsity for compressive data gathering,” *IEEE Transactions on Wireless Communications*, vol. 9, no. 12, pp. 3728–3738, Dec. 2010, doi: 10.1109/TWC.2010.092810.100063.

[21] N. Y. Yu, “Indistinguishability of compressed encryption with circulant matrices for wireless security,” *IEEE Signal Processing Letters*, vol. 24, no. 2, pp. 181–185, Feb. 2017, doi: 10.1109/LSP.2017.2647953.

[22] K. Hayashi, M. Nagahara, and T. Tanaka, “A user’s guide to compressed sensing for communications systems,” *IEICE Transactions on Communications*, vol. E96.B, no. 3, pp. 685–712, 2013, doi: 10.1587/transcom.E96.B.685.

[23] W. Chen, M. R. D. Rodrigues, and I. J. Wassell, “Distributed compressive sensing reconstruction via common support discovery,” in *2011 IEEE International Conference on Communications (ICC)*, Jun. 2011, pp. 1–5, doi: 10.1109/icc.2011.5962798.

[24] M. Lakshminarayana and M. Sarvagya, “OFCS: Optimized framework of compressive sensing for medical images in bottleneck network condition,” *International Journal of Electrical and Computer Engineering (IJECE)*, vol. 8, no. 5, pp. 2829–2838, Oct. 2018, doi: 10.11591/ijece.v8i5.pp2829-2838.

[25] M. A. Khajehnejad, W. Xu, A. S. Avestimehr, and B. Hassibi, “Weighted l1 minimization for sparse recovery with prior information,” in *2009 IEEE International Symposium on Information Theory*, Jun. 2009, pp. 483–487, doi: 10.1109/ISIT.2009.5205716.

[26] S. S. Chen, D. L. Donoho, and M. A. Saunders, “Atomic decomposition by basis pursuit,” *SIAM Journal on Scientific Computing*, vol. 20, no. 1, pp. 33–61, Jan. 1998, doi: 10.1137/S1064827596304010.

[27] E. Candes and J. Romberg, “l1-magic: Recovery of sparse signals via convex programming.” pp. 1–4, 2005, [Online]. Available: https://candes.su.domains/software/l1magic/downloads/l1magic.pdf

[28] Y. C. Pati, R. Rezaiifar, and P. S. Krishnaprasad, “Orthogonal matching pursuit: recursive function approximation with applications to wavelet decomposition,” in *Proceedings of 27th Asilomar Conference on Signals, Systems and Computers*, 1993, pp. 40–44, doi: 10.1109/ACSSC.1993.342465.

[29] W. Dai and O. Milenkovic, “Subspace Pursuit for Compressive Sensing Signal Reconstruction,” *IEEE Transactions on Information Theory*, vol. 55, no. 5, pp. 2230–2249, May 2009, doi: 10.1109/TIT.2009.2016006.

[30] T. Blumensath and M. E. Davies, “Iterative hard thresholding for compressed sensing,” *Applied and Computational Harmonic Analysis*, vol. 27, no. 3, pp. 265–274, Nov. 2009, doi: 10.1016/j.acha.2009.04.002.

[31] I. Daubechies, M. Defrise, and C. De Mol, “An iterative thresholding algorithm for linear inverse problems with a sparsity constraint,” *Communications on Pure and Applied Mathematics*, vol. 57, no. 11, pp. 1413–1457, Nov. 2004, doi: 10.1002/cpa.20042.

BIOGRAPHIES OF AUTHORS

Mathiyalakendran Aarthi Elaveini received her B.E degree in Electronics and Communication Engineering from Madurai Kamaraj University, Tamil Nadu, India, and her M.E degree in Embedded Systems Technologies from Anna University, Chennai, India in 2004 and 2012, respectively. She is currently pursuing her Ph. D at SRM University. She is currently working as an Assistant Professor in the Department of ECE, SRM Institute of Science and Technology, Ramapuram, Chennai, India. Her research interests are in the areas of wireless communication systems, image processing, and visible light communication. She can be contacted at email: aarthim@srmist.edu.in.

Deepa Thangavel received her B.Tech. degree in Electronics and Communication Engineering from Madras University, Chennai, India, and her M. Tech degree in Communication Engineering from VIT, Vellore, Chennai, India in 2004 and 2006, respectively. She completed her Ph. D in 2015. She is currently working as an Associate Professor in the department of ECE, SRM Institute of Science and Technology, Chennai, India. She has more than 19 publications in SCI/SCOPUS indexed journals and 22 proceedings in international and national conferences. She is currently supervising 6 Ph.D students. She is an active participant in both academic and research activities. Her research interests are in the areas of wireless communication systems, signal processing, visible light communication, multicarrier, and spread spectrum techniques for 5G communication. She can be contacted at email: deepat@srmist.edu.in.